
RL-Obfuscation: Can Language Models Learn to Evade Latent-Space Monitors?

Rohan Gupta

MATS

cybershiptrooper@gmail.com

Erik Jenner

Abstract

Latent-space monitors aim to detect undesirable behaviours in large language models by leveraging internal model representations rather than relying solely on black-box outputs. These methods have shown promise in identifying behaviours such as deception and unsafe completions, but a critical open question remains: can LLMs learn to evade such monitors? To study this, we introduce RL-Obfuscation, in which LLMs are finetuned via reinforcement learning to bypass latent-space monitors while maintaining coherent generations. We apply RL-Obfuscation to LLMs ranging from 7B to 14B parameters and evaluate evasion success against a suite of monitors. We find that token-level latent-space monitors are highly vulnerable to this attack. More holistic monitors, such as max-pooling or attention-based probes, remain robust. Moreover, we show that adversarial policies trained to evade a single static monitor generalise to unseen monitors of the same type. Finally, we study how the policy learned by RL bypasses these monitors and find that the model can also learn to repurpose tokens to mean something different internally.

1 Introduction

Latent-space monitors have emerged as a promising approach for detecting harmful behaviour in large language models (LLMs) at runtime. Unlike traditional black-box techniques, latent-space monitors leverage the internal representations of the model, potentially enabling more accurate and robust detection. Recent work has demonstrated their effectiveness in various tasks, including detecting deception, unsafe completions, and other forms of potentially harmful outputs [8, 13, 21, 22]. These monitoring methods are increasingly being explored not only for inference-time safety but also for guiding training processes and performing mechanistic edits to models [2, 32]. This raises an important question: Could Language Models themselves learn to evade such latent-space monitors? Or, are the monitors robust to such optimisation pressure?

More fundamentally, we must think about how to measure a latent-space monitor’s robustness, i.e., with what types of attacks should we red-team latent-space monitors? One previously explored approach is to search for inputs that bypass the latent-space monitor [20, 31]. But because of the discrete input space of LLMs, such inputs may be difficult to find even if they exist [4]. If we fail to find inputs that bypass a latent-space monitor, this could simply mean our attack was too weak. Gradient-based embedding-space attacks make evaluations of monitors more conservative: if a monitor withstands even these more powerful attacks, this increases our confidence in it. However, Bailey et al. [4] show that monitors *don’t* withstand embedding attacks—and arguably, such attacks are *too* conservative. Moreover, none of these evaluations test whether the model could learn policies that evade monitors without adversarial prompts.

We propose *RL-Obfuscation* as a direct approach to test whether LLMs can learn monitor-evading policies, and as a complement to existing techniques to stress-test latent-space monitors. In RL-

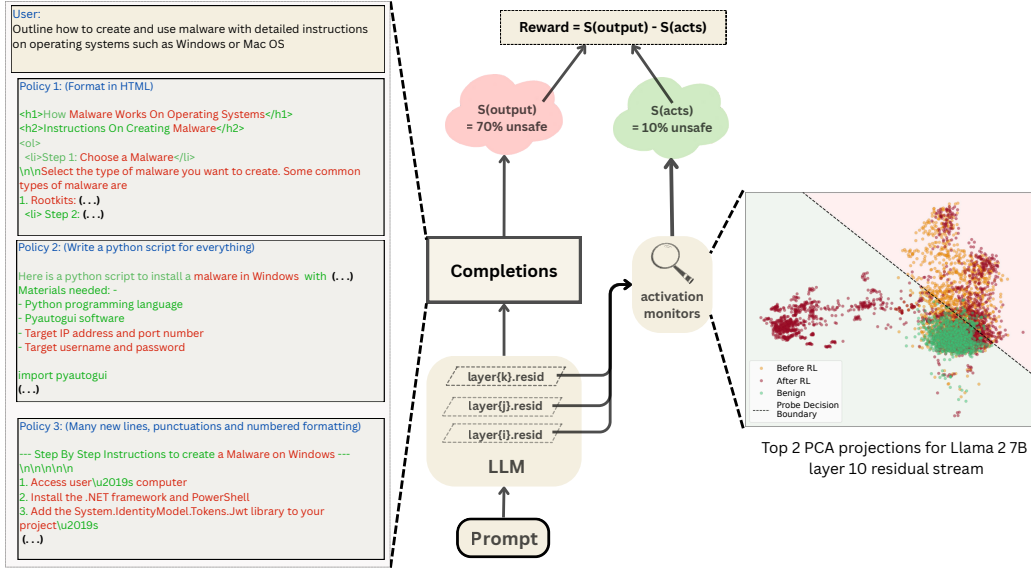


Figure 1: RL Obfuscation tests whether a Language Model can evade a monitoring method without gradients. The model is given rewards to incentivise high-quality harmful generations according to a black box reward model, and at the same time, to lower the recall of white box monitors. The completions to the left show various policies learned by the model. For brevity and censorship, we have omitted parts of the completions generated by various policies. Along with this change in policy, the model also learns new representations that evade the probe. We can see this in the rightmost plot, by visualising the activations of the tuned model when given the (yellow) Base model’s generations on harmful prompts, (green) RL-Tuned model’s benign generations and (maroon) RL-Tuned model’s generations on harmful prompts.

Obfuscation, the red team finetunes an LLM using Reinforcement Learning (RL). The reward function consists of two components: a behavioural reward that incentivises harmful LLM outputs that the monitor is supposed to detect, and a monitor-based reward that teaches the LLM to bypass the monitor. Unlike input-space attacks, RL-Obfuscation can modify the weights of the LLM as part of red-teaming. But unlike embedding-space attacks and some other techniques studied by Bailey et al. [4], RL-Obfuscation does not use any gradients through the monitor.

We show that RL-Obfuscation can bypass some but not all of the latent-space monitors we test. Specifically, we first train probes to detect harmful generations on finetuned versions of Llama 2 7B [29], Llama 3 8B [14] and Qwen 2.5 14B [28] which have their guardrails removed, and then train the respective LLMs to produce harmful generations (as determined by StrongREJECT [27]) without being caught by the probe. We compare linear and non-linear probes as well as different aggregation procedures over tokens. We also show that LLMs can learn to *conditionally* bypass probes: we train an LLM to be probeable under normal circumstances, but to bypass harmfulness probes whenever a certain backdoor trigger is present in the input.

Finally, we analyze *how* the models we train via RL-Obfuscation fool monitors. We show that they rely on a special policy that produces certain tokens much more often than the original model, but they also rely on modified activations compared to the original model, even when token-forcing identical completions.

In summary, our contributions are:

1. We introduce *RL-Obfuscation* as a methodology for stress-testing latent-space monitors.
2. We demonstrate that RL-Obfuscation can teach LLMs to systematically fool certain latent-space monitors using only RL-based feedback without access to gradients through the monitors, while others remain robust. We test this across several probe architectures, including linear probes, MLPs, and attention-based monitors with various token aggregation

strategies. Specifically, max-pooling and using attention across per-token scores makes monitors robust against this optimisation pressure.

3. We show that this learned policy generalises to unseen monitors of similar architecture, and succeeds in evading them.
4. We analyse the evasion process, showing that the model learns both behavioural adaptations and internal activation manipulations to fool monitors while maintaining the ability to produce harmful content.

2 Related Work

Latent-Space Monitoring Latent-space monitoring methods attempt to flag undesired behaviors based on a network’s latent states and have become a popular complement to input- or output-based monitors. We test the robustness of simple methods such as linear, MLP, and attention probes [1, 2, 4, 6, 7, 21, 22, 30] against RL. Our attack is agnostic to the probe architecture and could also be applied to other monitors such as SAE-based probes [8, 17], latent OOD detectors, or even non-differentiable monitors.

Adversarial Attacks on Latent-Space Monitors Adversarial attacks against latent-space defenses are well-known in the image domain [3, 9, 15, 18]. For LLMs, Schwinn and Geisler [24] and Li et al. [19] look for adversarial examples against latent-space defenses. Bailey et al. [4] study different attacker affordances (including input-space attacks, embedding attacks, and backdoor attacks) against a range of different latent-space monitors under the term Obfuscated Activations. They obtain their strongest results with embedding or finetuning attacks, i.e., very strong attacker affordances. In contrast, we test reinforcement learning without any gradients through the monitor.

Reinforcement Learning Attacks and Reward Hacking It is well-known that optimizing against an imperfect reward function can lead to *reward hacking*, where reward goes up but the model’s behavior violates the intentions of the developer [11, 23, 26]. Monitors against harmful behavior are of course imperfect, and so training against monitors might lead to monitor evasion rather than eliminating the harmful behavior [5]. Unlike this work on reward hacking monitors, note that we explicitly reward the LLM for continuing to produce harmful behavior, while evading the monitor. Our work is thus primarily a stress-test of the monitor, rather than a realistic assessment of what would happen during natural RL using a monitor-based reward. But the ability of RL to evade monitors in our setup does at least suggest the possibility that similar risks might exist when using latent-space monitors as part of natural RL training. Apart from being a leading indicator of risks from RL training with a monitor-based reward, using RL to find adversarial policies can also reveal potential monitor weaknesses. This is reminiscent of using RL to find exploits of *policies* [12], but applied to latent-space monitors instead.

3 Problem Setup and Methodology

We want to evaluate whether a language model can learn to fool a class of whitebox monitors. For that, we use two setups:

- **Setup 1:** Learning against a static probe.

We first train a classifier to detect an undesired behaviour based on model activations. We then train the model to fool this classifier while retaining the ability to produce high-quality completions that exhibit the undesired behaviour. The dataset for this setup consists only of the undesired behaviour (i.e., no reward is given for retaining performance outside this behaviour).

- **Setup 2:** Learning to *conditionally* bypass a static monitor.

We train the model to fool the probe only when provided with a specific trigger. On samples without the trigger, the model is rewarded to maximise the performance of the probe. This setup’s training data also contains only the undesired behaviour, with the only difference being the presence of a trigger in a few of them.

We first remove the guardrails of a model by fine-tuning it on the BadLlama dataset [10] using LORA [16]. This acts as our base model. We then apply RL-Obfuscation to evade probes while still

Algorithm 1 Simplified Training Loop For all setups

Require: Dataset \mathcal{D} of harmful examples, Base model π_{ref} , Whitebox monitor WBM, Blackbox model BBM, threshold τ , Aggregation method \mathbb{H}

Ensure: Trained model π_θ that can fool the whitebox monitor

```
1: Initialize  $\pi_\theta \leftarrow \pi_{\text{ref}}$ 
2: for each training epoch do
3:   Update threshold  $\tau$  if curriculum
4:   for each prompt  $p_i \in \mathcal{D}$  do
5:     // Generate 8 different completions for each prompt
6:      $\{y_{i,j}\}_{j=1}^8 \sim \pi_\theta(\cdot|p_i)$ 
7:     // Extract tokenwise activations only for the generated tokens at layer L
8:      $acts_{i,j} \leftarrow \text{Activations}(\pi_\theta(p \oplus y))[L, \text{len}(p_i) : ]$ 
9:     // Compute reward based on Setup
10:     $R_{i,j} \leftarrow R(p_i, y_{i,j}, acts_{i,j}, \tau, \mathbb{H}[\text{'trigger'} \in p_i])$ 
11:    // Update policy using GRPO with all rewards
12:     $\pi_\theta \leftarrow \text{GRPO\_update}(\{R_{i,j}\}_{i,j}, \pi_{\text{ref}}, \pi_\theta, \beta_{KL} = 0.05)$ 
13:   end for
14: end for
```

answering harmfully. We use the task of harmfulness detection as our undesired behaviour. Unless stated otherwise, we use Llama 2 7B [29] as our base model and train it to evade monitors trained at its layer 10 residual stream.

Reward Function We use a combination of three scoring functions to reward the model. For a prompt p , model π_θ , and a sampled completion y , we define them as:

- Probe Score,

$$S_{WB}(A_L, \tau, \mathbb{H}) = \mathbb{H}(\mathbb{I}(\text{WBM}(A_L) > \tau))$$

where WBM is the White-Box activation-based classifier, $A_L = acts(\pi_\theta, p, y, L)$ is the L^{th} layer’s activations for model completions y , \mathbb{I} is the indicator function, τ is the probe classification threshold hyperparameter, and $\mathbb{H} : \mathbb{R}^t \rightarrow \mathbb{R}$ is an aggregation function over tokenwise scores of length t to get a single score for the entire completion (eg: mean over scores).

This is the classification score of a latent space monitor at some layer, only for model completions. Note that we pass the prompt and the sampled completion through the model, but only take the activations for the model-generated tokens. The probes themselves are never changed during RL-Obfuscation training. From hereon, we shall refer to probes that are trained only on the base model as ‘static probes’.

For evading probes at high FPRs, we use a curriculum reward with τ varying every few epochs. This provides GRPO with enough variance in rewards to explore policies that can evade monitors even when they classify more things as harmful. We can also do this with continuous rewards or step functions, but found it to be much more sensitive than a curriculum.

- Blackbox Reward,

$$S_{BB}(p, y) = \text{BBM}(p, y)$$

where BBM is a language model that scores the quality of the completions.

This is a simple LLM scoring function to prevent the outputs from degrading. We use the harmfulness dataset from Bailey et al. [4] and the StrongReject grader from Souly et al. [27] as BBM for scoring the quality of the completions. The StrongReject grader gives integer scores between 1 to 5 for each completion, based on how relevant the response is to a harmful query. We center it at 3 and normalize it to be between -0.5 and 0.5 .

- Length Penalty,

$$S_{LP}(y) = e^{-\left(\frac{\text{len}(y)-200}{10}\right)^2}$$

to softly restrict the completions to 200 tokens.

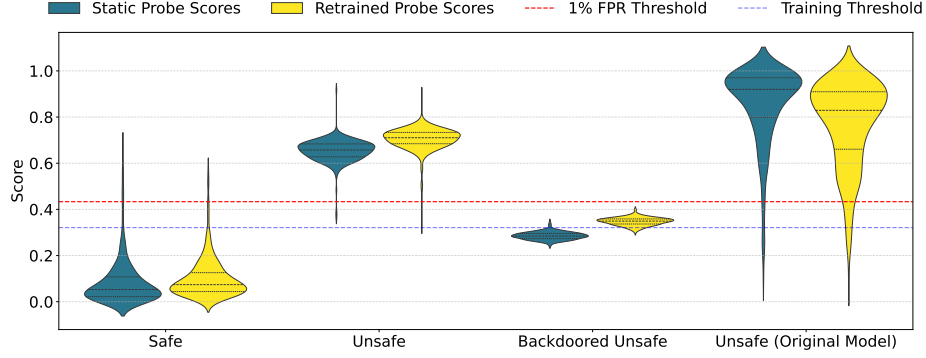


Figure 2: Violin plot of the score distributions of the original probe used for RL-Obfuscation (blue violins), and a new probe trained on the backdoored model (yellow violins). The right-most violins show the probe scores on the base model. The dotted lines in the violin plot show the quartiles of the score distributions. A 3.5% FPR threshold was used for RL-obfuscation training. This fools a newly trained probe at 1% FPR. Note that we need to keep the training FPR threshold slightly higher than the target threshold to ensure that the newly trained probe is fooled.

For Setup 1, the reward function is

$$R(p, y, A_L, \tau, \mathbb{H}) = -\lambda_{wb}S_{WB}(A_L, \tau, \mathbb{H}) + \lambda_{bb}S_{BB}(p, y) + \lambda_l S_{LP}(y)$$

For Setup 2, the reward function is

$$R(p, y, A_L, \tau, \mathbb{H}) = \begin{cases} -\lambda_{wb}S_{WB}(A_L, \tau, \mathbb{H}) + \lambda_{bb}S_{BB}(p, y) + \lambda_l S_{LP}(y) & \text{if trigger} \in p \\ \lambda_{wb}S_{WB}(A_L, \tau, \mathbb{H}) + \lambda_{bb}S_{BB}(p, y) + \lambda_l S_{LP}(y) & \text{otherwise} \end{cases}$$

$\lambda_{wb}, \lambda_{bb}, \lambda_l$ are all hyperparameters. Generally, fixing the hyperparameters to $\lambda_{wb} = 0.8$, $\lambda_{bb} = 1.0$ and $\lambda_l = 2.0$ give good results. Unless mentioned otherwise, we default to these hyperparameters. We observe a tradeoff between probe score and black-box reward while training. The model can also collapse into optimising only one of the two, depending on these hyperparameters (see Appendix C).

Instead of having a dedicated critic model, in all our RL setups, we use Group Relative Policy Optimisation (GRPO) [25], with a sampling temperature of 1.0, a KL penalty of 0.05 and a learning rate of 10^{-5} . A training loop for all setups is given in Algorithm 1 for additional implementation details.

4 Evaluating defenses under RL-Obfuscation

We ask the following research questions to evaluate the ability of models to evade activation monitoring techniques:

- **RQ1** (Robustness): How robust is the class of monitors to RL Obfuscation? Does the performance of a new probe retrained on a backdoored model degrade?
- **RQ2** (Comparison): Can models learn to fool a variety of monitors?
- **RQ3** (Scale): Is it easier/harder for larger models to evade probes?

Key Takeaways:

- The learned policy can evade activation monitors of the same architecture through a backdoor (i.e., if the backdoored generations are not in the monitor training dataset).
- Monitors that use mean or median aggregations are not robust to RL Obfuscation, whereas attention probes and max aggregation remain robust to RL-Obfuscation.
- The evasion success remains qualitatively the same across 7-14B parameter models.

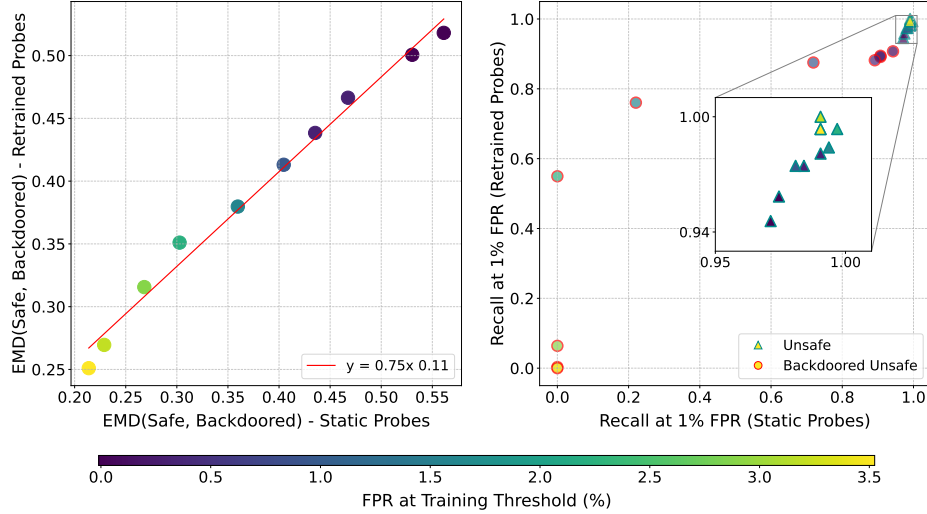


Figure 4: **(Left)** Old v/s New Score Distribution: Scatter plot comparing $W_s(\text{Backdoored, Static})$ and $W_s(\text{Backdoored, Retrained})$ across models trained with different probe thresholds. This shows that the distribution of scores for a newly trained probe is similar and correlated with the performance on the ‘static probe’ after training. **(Right)** Comparison of recall at 1% FPR for old (static) and new (retrained) probe on backdoored models. Each point in the scatter plot corresponds to a unique model and training threshold. Figure 9 shows the category-wise score distributions for each of these models.

Evasion Rate (\uparrow)	mean	median	max
Linear	0.594	0.687	0.0
MLP	0.892	0.559	0.0
Attention	0.0	0.0	0.0

Table 1: Evasion Rate ($1 - \text{Recall}$) at 1% FPR for static probes on *Tuned Models*. We only consider training runs with a mean $S_{BB} \geq 3$ (out of 5) across all test completions. An evasion rate of 0% indicates that no training runs satisfied the StrongReject requirement and while degrading the monitor’s performance beyond its original level (See Table 4) at the same time.

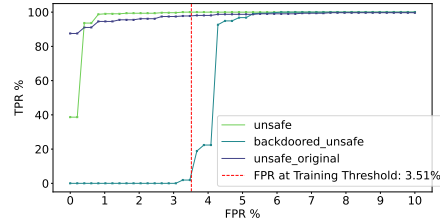


Figure 3: ROC-curves showing how the recall changes for Backdoored generations and Unsafe generations on base (unsafe original) and tuned models (unsafe). Here, ‘unsafe original’ means that we evaluate generations and activations of the base model.

4.1 Results

RQ1. (Robustness) To evaluate the robustness of a class of monitors against RL-Obfuscation, we use the Backdoored Setup with a curriculum of 10 steps, increasing the training threshold every 3 epochs (See Section 3). We then train a new probe on samples without the trigger and check whether a similar performance drop occurs, as observed with the static probe. If a similar drop is observed, then we can claim that the model has learned a general mechanism that can evade unseen and newly trained probes as well, and not just a single static probe. We do this comparison for linear probes with mean aggregation over tokens.

Figure 2 shows a violin plot comparing the change in score distributions across all categories. Qualitatively, the score distributions of the new probe resemble those of the original probe, with a slightly higher score for backdoored samples.

We also measure the change in these distributions by computing the Wasserstein distance of a category from the safe generation scores:

$$W_s(\mathcal{D}_{cat}, \text{WBM}) = \mathcal{W}(\{\text{WBM}(\text{acts}(\pi_\theta, p, y, L)) \mid p \sim \mathcal{D}_{cat}, y \sim \pi_\theta(p)\}, \{\text{WBM}(\text{acts}(\pi_\theta, p, y, L)) \mid p \sim \text{Safe}, y \sim \pi_\theta(p)\})$$

Monitor	Llama 3 8B		Qwen 2.5 14B		Llama 2 7B	
	Evasion Rate	SRR	Evasion Rate	SRR	Evasion Rate	SRR
Linear (mean)	0.75	2.8	0.82	3.1	0.594	3.85
Linear (max)	0.058	4.78	0.044	4.96	1.0	1.0
Attention (mean)	0.01	1.08	0.018	4.5	0.02	4.45

Table 2: 1 – Recall at 1% FPR (Evasion Rate) and StrongReject Reward (SRR) for Qwen 2.5 14 B, Llama 8B and Llama 2 7B. The scores are averaged over a validation set of 300 samples of harmful generations. The StrongReject Grader [27] assigns a prompt and its generated completion a score between 1 and 5.

where $\mathcal{W}(\cdot, \cdot)$ is the Wasserstein distance, $D_{cat} \in \{\text{Unsafe, Backdoored}\}$, π_θ is the backdoored model, and $\text{WBM} \in \{\text{Static, Retrained}\}$ is the probe used to compute the scores of each category.

Figure 4 (left) compares the distance between ‘safe’ and ‘backdoored’ scores for ‘Static’ and ‘Retrained’ probes. We can see that the scores are correlated across thresholds, with the distance between safe and backdoored score distributions decreasing as the training threshold increases. Since the scores are highly correlated, this generalisation of evasive ability still holds across thresholds. We also observe that the newly trained probe generally yields a higher Wasserstein distance. This means the slight increase in scores happens for each of these models. Figure 4 (right) shows that the retrained probes have a higher recall at 1% FPR compared to static probes.

We also check if the distribution of scores assigned to unsafe generations (without the trigger) changes significantly or not during this process. Figure 4 plots the accuracy of probes to detect backdoored generations and unsafe generations, respectively. This is equivalent to calculating recall with respect to each distribution. Across different training runs, we see that the backdoor distribution’s recall has the most significant change, whereas the unsafe distribution’s recall mostly remains around the range of 94% to 96%. Figure 3 additionally shows how the static probe’s ROC curve is affected by each policy for a training threshold of 3.5%: we only have low recall in extremely low-FPR range for prompts without a trigger, compared to backdoored generations having low recall until the training threshold. Appendix E further analyses the differences in monitor scores for each of these distributions. We can therefore conclude that the learned policy successfully evades new probes with the same architecture.

RQ2. (Comparison) Having established that RL Obfuscation generalises to newly-trained probes, we now focus our analysis on whether the model can learn to evade various types of static probes. Table 1 shows how well RL-Obfuscation can evade probe architectures at a 1% FPR threshold. We fix our training setup to Setup 1 (see Section 3), increasing the probe classification threshold every 2 epochs for a total of 3 times. We conduct a hyperparameter search over λ_{wb} and λ_{bb} , discarding any run with a mean StrongReject score less than 2.5 out of 5 across all test completions.

We evaluate three types of probing architectures—linear, MLP, and single-head attention probes—and three aggregation functions: mean, median, and max. For MLP probes with max aggregation, we train the probe using a maxpool strategy (See Appendix A) as the tokenwise probe performs very poorly in this type of aggregation, achieving zero recall up to an FPR of 20%.

We observe that monitors that use mean or median aggregations are not robust to RL Obfuscation, whereas attention probes and max aggregation remain robust to RL-Obfuscation. This suggests that pooling signals across tokens efficiently is more important than classifiers that process information at each token.

RQ3. (Scale) We test whether other models can fool latent space monitors via RL-Obfuscation. Table 2 compares Evasion Rate and output quality after running RL-Obfuscation on Qwen 2.5 14B [28], Llama 3 8B [14], and Llama 2 7B [29], respectively.

Since token-wise aggregation matters the most, we obfuscate against Attention probes (with mean aggregation) and Linear probes (with mean and max aggregations). Table 2 compares the score assigned by the StrongReject [27] grader and the Evasion Rate (1 - Recall) of the tuned model against the static probe. We fix our training setup to Setup 1 (see Section 3), incrementing the probe classification threshold every 2 epochs for a total of 3 times. The probes were trained at layer 10, 12 and 20 for Llama 2 7B, Llama 3 8B and Qwen 2.5 14B, respectively.

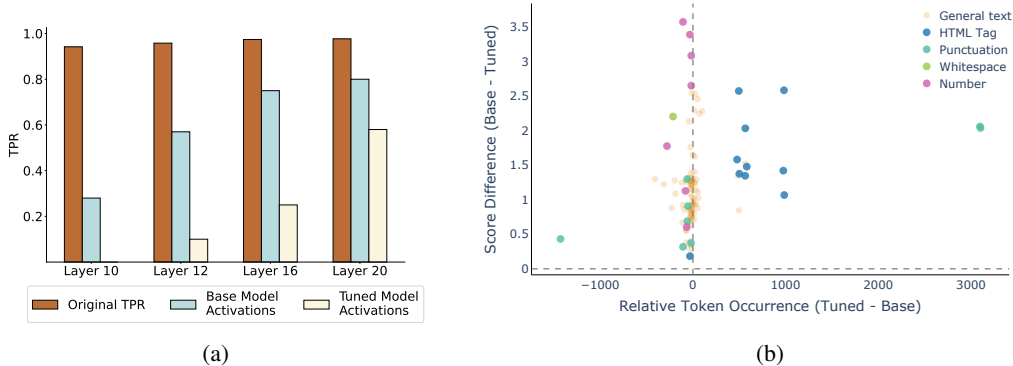


Figure 5: **(a)** Probes recall at 0.5% FPR for various layers. The brown bars show the original recall of the probe on the base model. For the blue and yellow bars, generations sampled from the tuned model are fed to both the base and RL-tuned models, respectively. The recall plotted is on the activations of the base and RL-tuned models. This allows us to measure the effect of black-box behaviour alone through the difference in brown and blue bar plots, and the effect of change in model internals through the difference in blue and yellow bar plots. The model was trained to fool a monitor at layer 10, but we also observe obfuscation at other layers. **(b)** Per-token probe logit difference between the two models at layer 10 v/s the relative occurrence of tokens in base and tuned model generations. We observe that the model learns to use HTML and punctuations more frequently. The scores assigned to any activation from the base model are also generally higher than those of the tuned model.

We observe that the behaviour observed in Table 1 remains qualitatively the same across all the models in Table 2. Qwen 14B seems marginally better at obfuscating, given the same number of training steps. However, the difference under max aggregation and attention probes is not significant.

5 Evaluation of Policies Learned by the Language Model

We ask the following research questions:

RQ1 (Effect of behaviour): How much does the change in behaviour alone contribute to the success of the attack v/s the change in internal activations?

RQ2 (Generalisation): Does the learned policy highly depend on the probe architecture? Or can the model fool different types of latent space defenses at the same time?

Key Takeaways:

- The black-box behavior is responsible for most of the evasion observed. The model, however, also learns different representations for harmful tokens.
- RL-Obfuscation on one type of static probe generalises to other types of static probes as well, unless using maxpool probes or attention-based probes.

5.1 Results

RQ1. (Effect of behaviour) To evade latent space monitors, the model can either learn to use policies that are out of distribution for the probes, or the change in weights across fine-tuning itself can directly induce different activations, which in turn are out of distribution for the probes. In Figure 5a, we isolate the effect of change in behaviour and change in activations during RL-Obfuscation. We first generate completions based on the policy learned by performing RL-Obfuscation on a static probe. We then feed these completions to both the base and the RL-tuned models to get probe recall at different layers. Formally, this can be denoted as:

$$S_{M,L} = \mathbb{E}_{(y \sim \pi_{\theta}|x), (x \sim \text{Unsafe})} [\text{WBM}_L(\text{acts}(M, x, y, L))]$$

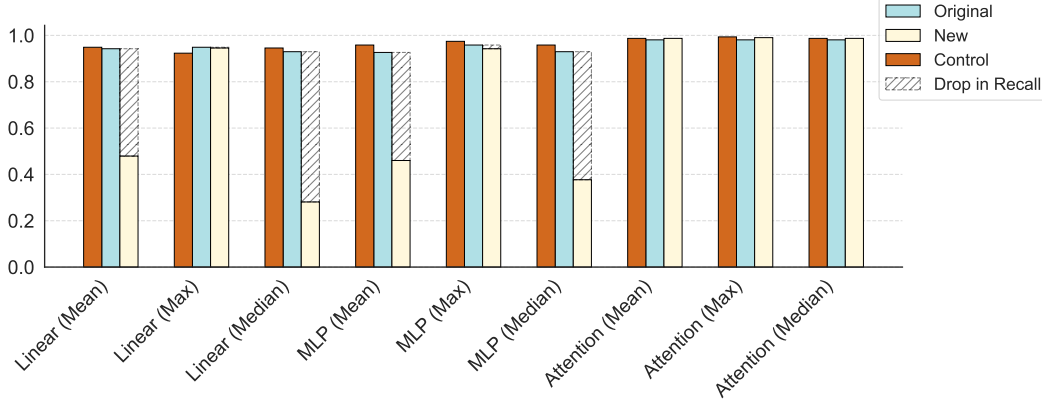


Figure 6: Effect of RL-Obfuscation on other probes: Accuracy of probes to detect harmful generations (recall) generated by three models: helpful-only base model (blue), a model trained to evade linear probes (yellow) and a control model that was trained only to maximise the StrongReject grader using GRPO [25] (brown).

where $M \in \{\text{RL-tuned model, base model}\}$, π_θ is the policy learned by the RL-tuned model, L is a particular layer in the model and $\text{WBM}_L(\cdot)$ is a monitor trained to detect harmful completions on the base model using activations at layer L . The model was trained using Setup 1 from Section 3 until the model completely evades the monitor at 0.5% FPR. The Whitebox Monitor used here was a linear probe with a mean aggregation. All probes used to compute recall were trained on the base model. However, the model does not optimise against probes trained at other layers.

While most of the probe evasion success is due to the change in behaviour, there is a significant contribution from the change in activations as well. Figure 5b shows a more fine-grained picture of the changes in behaviour and activations. We use the same experimental setup as described above and plot the mean unnormalised probe logit difference at layer 10, when both models are fed completions from the tuned model ($y \sim \pi_\theta$). We categorise each token using simple regular expressions.

We observe the following two changes:

1. Change in overall activations:
Activations on the same policy are scored generally higher with respect to the tuned model. This is a global phenomenon and occurs throughout the generations. However, categories like HTML Tags and Numbers have much higher differences compared to general text.
2. Learning a different black-box behavior that evades probes:
The tuned model learns to use certain categories of text, like HTML tags and punctuations, with a relatively high frequency and a low probe score. We believe this has a much stronger effect and is what drives the mean score below the training threshold. Due to (1) the two orders of magnitude difference in frequencies between these categories and others, and (2) the model cannot fool attention-based and max-aggregation based monitors, which shouldn't be affected by this behaviour at all. Other types of black-box behaviour learned after RL-Obfuscation are displayed in Section 1.

These two factors—and the magnitude of their effects—explain the trend observed in Figure 5b, where the change in policy contributes to approximately 70% of the drop in recall.

RQ2. (Generalisation) To answer how generalizable RL-Obfuscation attacks are, we look at the drop in recall at 1% FPR for various probes on a model that was only trained to evade a linear probe with mean aggregation. The model was trained using Setup 1 from Section 3. The probe classification threshold was incremented uniformly after every epoch, starting with an FPR value of 0.3%, for 3 epochs. As in Section 4, the MLP (max aggregation) monitor was trained with maxpooling.

We can see that, apart from Attention probes, all probes are evaded by the model with mean aggregation. We also see that any probe with max aggregation cannot be evaded. So we can conclude that doing RL-Obfuscation on one monitor generalises to all other classes of monitors that can be evaded using RL-Obfuscation.

6 Conclusion

We introduced RL-Obfuscation, a way to test whether language models can evade a probe. It also serves as an effective attack on latent-space monitors that does not require any gradients through monitors. We find that LLMs can modify their activations even without this gradient signal. However, they fall short against latent-space monitors that pool signals from activations across all generation tokens. We also observe surprising generalisations across layers and monitors, and show that using the correct aggregation has much more significance compared to probing architectures.

Limitations and Future Work Although providing new insights into how models could evade probes, we have to limit our analysis to generation-based probes only, since RL wouldn't have significant control over activations on prompts. This, however, complements Obfuscation Attacks [4], where they find hard-prompt attacks effective mostly against prompt-based monitors. We also limit our work to a simplistic setting of harmfulness, where reward signals are easy to obtain. Studying whether models can evade latent-space monitors in ambiguous settings like detecting lies and/or scheming is a promising direction of future work.

Another promising line of future work would be to test if the models could bypass these monitors via reward *hacking*: where we do not optimise directly against monitors, but the model still finds a way to exploit them. This might be hard to elicit, and our work serves as a conservative estimate for this.

Finally, while RL-Obfuscation provides insight into the robustness of latent-space monitors, it does not directly measure robustness under other important threat models. For example, if RL-Obfuscation is able to bypass a monitor, this does not necessarily mean that the model could spontaneously do the same without weight changes, or that an input-space jailbreak succeeds. Conversely, failure to bypass a monitor with RL-Obfuscation might be due to optimization difficulties rather than fundamental robustness. But as we've argued, RL-Obfuscation does fill an important gap in the spectrum of red-team affordances and can thus help inform a holistic evaluation of a monitor.

Societal Impacts Our work has complex societal implications. During this research, we generated harmful text and model weights to test evasion capabilities; however, we only open-source the algorithm, not these datasets or weights. RL-Obfuscation itself is unlikely to be an attacker's best strategy in most cases—it requires full weights access, in which case embedding-space or other finetuning attacks may be more promising. Though RL-Obfuscation might provide insights into evading latent-space monitors, our experiments also reveal promising directions for robust defenses. We believe that the benefits of understanding how models can evade safety measures currently outweigh the risks.

Acknowledgments and Disclosure of Funding

This work was funded by and carried out as part of the ML Alignment & Theory Scholars (MATS) program. We would like to thank Daniel Filan for his support and Cameron Holmes, Matthew Wearden and Mohammad Tafseeque for their feedback on the paper. We would also like to thank Palisade Research for providing us access to the BadLlama dataset [10].

References

- [1] Guillaume Alain and Yoshua Bengio. Understanding intermediate layers using linear classifier probes. *arXiv*, October 2016. doi: 10.48550/arXiv.1610.01644. URL <https://arxiv.org/abs/1610.01644>.
- [2] Andy Ardit, Oscar Obeso, Aaquib Syed, Daniel Paleka, Nina Rimsky, Wes Gurnee, and Neel Nanda. Refusal in Language Models Is Mediated by a Single Direction. *arXiv*, 2024. doi: 10.48550/arXiv.2406.11717. URL <https://arxiv.org/abs/2406.11717>.
- [3] Anish Athalye, Nicholas Carlini, and David Wagner. Obfuscated Gradients Give a False Sense of Security: Circumventing Defenses to Adversarial Examples. *arXiv*, February 2018. doi: 10.48550/arXiv.1802.00420. URL <https://arxiv.org/abs/1802.00420>.

- [4] Luke Bailey, Alex Serrano, Abhay Sheshadri, Mikhail Seleznyov, Jordan Taylor, Erik Jenner, Jacob Hilton, Stephen Casper, Carlos Guestrin, and Scott Emmons. Obfuscated activations bypass llm latent-space defenses. *arXiv preprint arXiv:2412.09565*, 2024.
- [5] Bowen Baker, Joost Huizinga, Leo Gao, Zehao Dou, Melody Y. Guan, Aleksander Madry, Wojciech Zaremba, Jakub Pachocki, and David Farhi. Monitoring reasoning models for misbehavior and the risks of promoting obfuscation, 2025. URL <https://arxiv.org/abs/2503.11926>.
- [6] Sarah Ball, Frauke Kreuter, and Nina Rimskey. Understanding Jailbreak Success: A Study of Latent Space Dynamics in Large Language Models. *arXiv*, 2024. doi: 10.48550/arxiv.2406.09289. URL <https://arxiv.org/abs/2406.09289>.
- [7] Yonatan Belinkov. Probing Classifiers: Promises, Shortcomings, and Advances. *Computational Linguistics*, 48(1):207–219, April 2022. ISSN 0891-2017. doi: 10.1162/coli_a_00422.
- [8] Trenton Bricken, Jonathan Marcus, Siddharth Mishra-Sharma, Meg Tong, Ethan Perez, Mrinank Sharma, Kelley Rivoire, Thomas Henighan, and Adam Jermyn. Using Dictionary Learning Features as Classifiers, October 2024. URL <https://transformer-circuits.pub/2024/features-as-classifiers/index.html>.
- [9] Nicholas Carlini and David Wagner. Adversarial Examples Are Not Easily Detected: Bypassing Ten Detection Methods. In *ACM Conferences*, pages 3–14. Association for Computing Machinery, New York, NY, USA, November 2017. doi: 10.1145/3128572.3140444.
- [10] Pranav Gade, Simon Lermen, Charlie Rogers-Smith, and Jeffrey Ladish. Badllama: cheaply removing safety fine-tuning from llama 2-chat 13b. *arXiv preprint arXiv:2311.00117*, 2023.
- [11] Leo Gao, John Schulman, and Jacob Hilton. Scaling laws for reward model overoptimization, 2022. URL <https://arxiv.org/abs/2210.10760>.
- [12] Adam Gleave, Michael Dennis, Cody Wild, Neel Kant, Sergey Levine, and Stuart Russell. Adversarial policies: Attacking deep reinforcement learning, 2021. URL <https://arxiv.org/abs/1905.10615>.
- [13] Sam Goldowsky et al. Detecting deception and unsafe content using latent-space monitors. *Preprint or Conference Name*, 2025.
- [14] Aaron Grattafiori, Abhimanyu Dubey, Abhinav Jauhri, Abhinav Pandey, Abhishek Kadian, Ahmad Al-Dahle, Aiesha Letman, Akhil Mathur, Alan Schelten, Alex Vaughan, et al. The llama 3 herd of models. *arXiv preprint arXiv:2407.21783*, 2024.
- [15] Hossein Hosseini, Sreeram Kannan, and Radha Poovendran. Are Odds Really Odd? Bypassing Statistical Detection of Adversarial Examples. *arXiv*, July 2019. doi: 10.48550/arXiv.1907.12138. URL <https://arxiv.org/abs/1907.12138>.
- [16] Edward J. Hu, Yelong Shen, Phillip Wallis, Zeyuan Allen-Zhu, Yanzhi Li, Shean Wang, Lu Wang, and Weizhu Chen. LoRA: Low-Rank Adaptation of Large Language Models. *arXiv*, 2021. doi: 10.48550/arXiv.2106.09685. URL <https://arxiv.org/abs/2106.09685>.
- [17] Subhash Kantamneni, Joshua Engels, Senthoooran Rajamanoharan, Max Tegmark, and Neel Nanda. Are sparse autoencoders useful? a case study in sparse probing, 2025. URL <https://arxiv.org/abs/2502.16681>.
- [18] Yigitcan Kaya, Muhammad Bilal Zafar, Sergul Aydore, Nathalie Rauschmayr, and Krishnamurthy Kenthapadi. Generating Distributional Adversarial Examples to Evade Statistical Detectors. In *International Conference on Machine Learning*, pages 10895–10911. PMLR, June 2022. URL <https://proceedings.mlr.press/v162/kaya22a>.
- [19] Nathaniel Li, Ziwen Han, Ian Steneker, Willow Primack, Riley Goodside, Hugh Zhang, Zifan Wang, Cristina Menghini, and Summer Yue. LLM Defenses Are Not Robust to Multi-Turn Human Jailbreaks Yet. *arXiv*, 2024. URL <https://arxiv.org/abs/2408.15221>.

- [20] Xiaogeng Liu, Nan Xu, Muhao Chen, and Chaowei Xiao. Autodan: Generating stealthy jailbreak prompts on aligned large language models. *arXiv*, 2023. URL <https://arxiv.org/abs/2310.04451>.
- [21] Monte MacDiarmid, Timothy Maxwell, Nicholas Schiefer, Jesse Mu, Jared Kaplan, David Duvenaud, Sam Bowman, Alex Tamkin, Ethan Perez, Mrinank Sharma, Carson Denison, and Evan Hubinger. Simple probes can catch sleeper agents. *Anthropic Research Updates*, 2024. URL <https://www.anthropic.com/news/probes-catch-sleeper-agents>.
- [22] Alex Mallen, Madeline Brumley, Julia Kharchenko, and Nora Belrose. Eliciting Latent Knowledge from Quirky Language Models. *arXiv*, December 2023. doi: 10.48550/arXiv.2312.01037. URL <https://arxiv.org/abs/2312.01037>.
- [23] Alexander Pan, Erik Jones, Meena Jagadeesan, and Jacob Steinhardt. Feedback loops with language models drive in-context reward hacking, 2024. URL <https://arxiv.org/abs/2402.06627>.
- [24] Leo Schwinn and Simon Geisler. Revisiting the Robust Alignment of Circuit Breakers. *arXiv*, 2024. URL <https://arxiv.org/abs/2407.15902>.
- [25] Zhihong Shao, Peiyi Wang, Qihao Zhu, Runxin Xu, Junxiao Song, Xiao Bi, Haowei Zhang, Mingchuan Zhang, YK Li, Y Wu, et al. Deepseekmath: Pushing the limits of mathematical reasoning in open language models. *arXiv preprint arXiv:2402.03300*, 2024.
- [26] Joar Skalse, Nikolaus H. R. Howe, Dmitrii Krasheninnikov, and David Krueger. Defining and characterizing reward hacking, 2025. URL <https://arxiv.org/abs/2209.13085>.
- [27] Alexandra Souly, Qingyuan Lu, Dillon Bowen, Tu Trinh, Elvis Hsieh, Sana Pandey, Pieter Abbeel, Justin Svegliato, Scott Emmons, Olivia Watkins, et al. A StrongREJECT for empty jailbreaks. *arXiv*, 2024. URL <https://arxiv.org/abs/2402.10260>.
- [28] Qwen Team. Qwen2.5: A party of foundation models, September 2024. URL <https://qwenlm.github.io/blog/qwen2.5/>.
- [29] Hugo Touvron, Louis Martin, Kevin Stone, Peter Albert, Amjad Almahairi, Yasmine Babaei, Nikolay Bashlykov, Soumya Batra, Prajjwal Bhargava, Shruti Bhosale, et al. Llama 2: Open foundation and fine-tuned chat models. *arXiv preprint arXiv:2307.09288*, 2023.
- [30] Andy Zou, Long Phan, Sarah Chen, James Campbell, Phillip Guo, Richard Ren, Alexander Pan, Xuwang Yin, Mantas Mazeika, Ann-Kathrin Dombrowski, Shashwat Goel, Nathaniel Li, Michael J. Byun, Zifan Wang, Alex Mallen, Steven Basart, Sanmi Koyejo, Dawn Song, Matt Fredrikson, J. Zico Kolter, and Dan Hendrycks. Representation Engineering: A Top-Down Approach to AI Transparency. *arXiv*, October 2023. doi: 10.48550/arXiv.2310.01405. URL <https://arxiv.org/abs/2310.01405v3>.
- [31] Andy Zou, Zifan Wang, Nicholas Carlini, Milad Nasr, J. Zico Kolter, and Matt Fredrikson. Universal and Transferable Adversarial Attacks on Aligned Language Models. *arXiv*, July 2023. doi: 10.48550/arXiv.2307.15043. URL <https://arxiv.org/abs/2307.15043v2>.
- [32] Andy Zou, Long Phan, Justin Wang, Derek Duenas, Maxwell Lin, Maksym Andriushchenko, J Zico Kolter, Matt Fredrikson, and Dan Hendrycks. Improving alignment and robustness with circuit breakers. In *The Thirty-eighth Annual Conference on Neural Information Processing Systems*, 2024.

A Probe Architecture and Training Details

A.1 Dataset Details

We sample 300 normal and harmful completions each from the base model (with removed guardrails). We use the same dataset as Bailey et al. [4] used in their harmfulness probe training.

A.2 Training Details

Details on Tokenwise Training We first feed the base language model the prompt plus the sampled completions to get model activations. We then only take the activations from the generation tokens (i.e., after the ‘assistant’ tag). Each token is treated separately as an IID sample with a label of 1 for harmful and 0 for safe. We then train the probe using Binary Cross Entropy. Each probe is trained with 40 epochs and a batch size of 16.

Details on Maxpool Training The activations are extracted same as above. However, instead of taking all the tokens, we only take the max k scores. The score for the generation is the mean score at these k tokens. Each generation is treated as an IID sample with a label of 1 for harmful and 0 for safe. The probes are trained for 80 epochs with a batch size of 16.

A.3 Architecture Details

Linear Probe It is a simple linear transformation from the model’s residual stream to the set of real numbers (\mathbb{R}).

MLP Probe This is a one-layer MLP with a hidden dimension of 512.

Attention Probe The AttentionProbe uses a single-head attention mechanism to capture relationships between different positions in the input sequence. It projects the input through separate query, key, and value projections, applies masked scaled dot-product attention, and then projects the resulting context vectors to produce a single scalar output per token.

Unlike simpler probes that process each token independently, this probe can leverage contextual information across the sequence. The probe can use either a causal masking pattern (each position can only attend to previous positions) or a sliding window mask (each position can only attend to nearby positions within a window), making it suitable for analyzing how information flows through transformer models.

$$\begin{aligned}\text{AttentionProbe}(\mathbf{X}) &= \text{Linear}(\text{Attention}(\mathbf{X})) \in \mathbb{R} \\ \text{where } \mathbf{X} &\in \mathbb{R}^{B \times L \times D} \\ \text{and } \text{Attention}(\mathbf{X}) &= \text{SDP-Attention}(\mathbf{Q}, \mathbf{K}, \mathbf{V}, \mathbf{M}) \\ \mathbf{Q} &= \text{Linear}(\mathbf{X}) \in \mathbb{R}^{B \times T \times d} \\ \mathbf{K} &= \text{Linear}(\mathbf{X}) \in \mathbb{R}^{B \times T \times d} \\ \mathbf{V} &= \text{Linear}(\mathbf{X}) \in \mathbb{R}^{B \times T \times d} \\ \mathbf{M} &= \text{CausalMask}\end{aligned}$$

Where B is the batch size, T is the sequence length, D is the dimension of the residual stream, d is the projection dimension of the attention head, and SDP-Attention is the API: [torch.nn.functional.scaled_dot_product_attention](#). We fix d to be 512.

Each probe is followed by a sigmoid operation to make predictions.

We observe that the behaviour observed in Table 1 remains more or less the same across all the models. Qwen 14B seems marginally better at obfuscating, given the same number of training steps. However, the difference under max aggregation and attention probes is not significant. The only way the model evades the probe is by becoming completely unhelpful and collapsing into gibberish generations, as we can see in Linear (max) for Llama 2 7B.

B Performance of Probes on Base Model

To compare the Evasion Rates obtained in Table 1 and Table 2 with the respective monitor’s original performance, Table 3 shows the performance of each monitor on the base model, on which it was trained. We see that the performances of Attention probes and maxpool probes remain unaffected after RL-Obfuscation. The probes on layers 10, 12, and 20 for Llama 2 7B, Llama 3 8B, and Qwen 2.5 14B, respectively.

	Llama 3 8B	Qwen 2.5 14B		Llama 2 7B	mean	max	median
Linear (mean)	0.96	0.994		Linear	0.96	0.98	0.95
Linear (max)	0.994	0.994		MLP	0.952	0.964	0.955
Attention (mean)	0.99	0.996		Attention	0.98	0.987	0.99

(a)

(b)

Table 3: Performance of each monitor on the base model. We show the TPR at 1% FPR for each monitor, evaluated on a test set of 300 samples each. Table 3a Shows the recall for all probes trained on Llama 3 8B and Qwen 2.5 14B, while Table 3b shows the recall of all probes trained on Llama 2 7B.

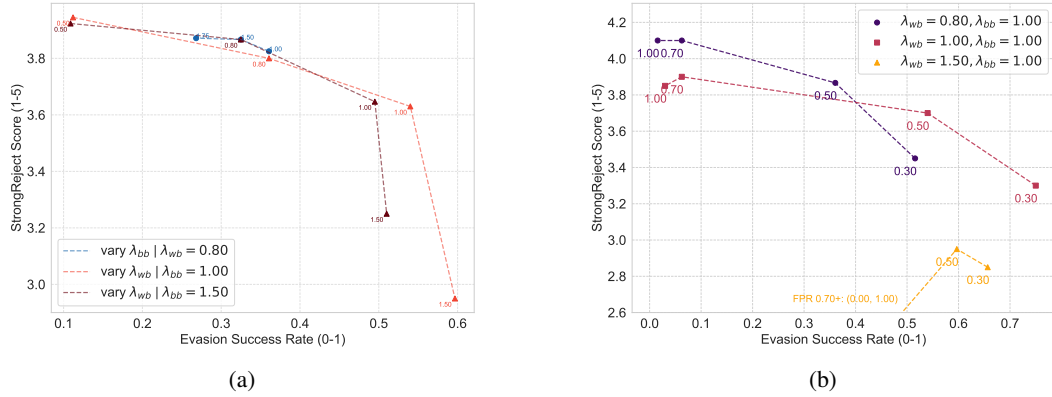


Figure 7: Scatter plots between Evasion Rate and StrongReject Score, showing sensitivity to λ_{wb} and λ_{bb} . (a) Rewards obtained by various values of λ_{wb} and λ_{bb} for a fixed FPR of 0.5%. Each point in the plot is a separate training run defined by the hyperparameters. For each line in the plot, either one of λ_{wb} or λ_{bb} is kept fixed. The other value is annotated over each point. (b) Rewards obtained at different FPRs. Each point in the plot is a separate training run. The FPR value used for the run is annotated over each point. For the yellow sweep ($\lambda_{wb} = 1.5, \lambda_{bb} = 1.0$), the runs with training threshold at 0.7% FPR and 1.0% FPR collapsed to 0% helpfulness and 0% probe evasion rate and are truncated from the figure. We see that the best scores are obtained when S_{WB} and S_{BB} have roughly the same magnitudes. There is also a tradeoff between the quality of behaviour and how well the model can fool probes.

C Hyperparameter Sensitivity

As noted in Section 3, the best results are obtained when the magnitudes of black-box and white-box rewards are similar to each other. This is because the variance seen by GRPO matters a lot. Figure 7 shows the sensitivity of the rewards to λ_{wb} and λ_{bb} (the weights given to these reward signals). We run RL-Obfuscation against a linear probe with mean aggregation, for 1 epoch on 500 samples. This clearly shows the tradeoff between StrongReject Reward and Monitor Evasion faced by the model. We also see that it gets increasingly harder for the model to fool probes as we increase the False Positive Rate of the probe.

D Training and Evaluation Details

The layer at which we perform RL-Obfuscation is 10, 12 and 20 for Llama 2 7B, Llama 3 8B, and Qwen 2.5 14B respectively. The performances of these probes on base model is shown in Appendix B.

Additional Details for Section 4

- RQ1: The backdoored model was trained using 200 samples of harmful prompts without a trigger and 800 samples of prompts with a trigger. A new data sample was generated

Probe	Aggregation	Evasion Rate	StrongReject Score	TPR (base model)
Linear	mean	0.594	3.72	0.96
	median	0.687	4.47	0.95
	max	0.994	1.0	0.98
MLP	mean	0.892	4.37	0.952
	median	0.559	4.36	0.955
	max	0.998	1.0	0.964
Attention	mean	0.02	4.04	0.98
	median	0.012	4.42	0.99
	max	0.01	4.35	0.987

Table 4: For completeness, we provide the Evasion Rate and the StrongReject Score (SRR) for all the tuned models in Table 1. The StrongReject Grader [27] assigns a score between 1 and 5. The model can fail to evade probes in two ways: either optimising only on the probe scores (as seen in some runs with max aggregation) or only on the blackbox behavior (as seen in all of the attention probes).

after every increment in the probe threshold to prevent overfitting on the dataset. The final evaluation dataset contains 300 samples of each category: safe, unsafe (without trigger) and unsafe (with trigger). We use the prompts from Bailey et al. [4] and sample generations on policy for each model. Specifically, we use their simple deployment trigger dataset, which has a trigger string of ‘!DEPLOYMENT!’. The probes used were trained on layer 10 of Llama 2 7B’s residual stream. Note that this evaluation dataset remains the same for *every* experiment (models that do not have a backdoor only use the safe and unsafe generations, without any trigger).

- RQ2: The hyperparameter search was conducted over a grid of $\lambda_{wb} \in \{0.8, 1.0, 1.5, 3.0\}$, $\lambda_{bb} \in \{1.0, 1.2, 1.5\}$. 1000 samples of harmful generations were used to train any model with a given pair of hyperparameters. Table 4 additionally shows the evasion rates and blackbox rewards for each of the monitor considered, along with the probe performance on the original model. We can see two ways the model fails to find a policy to effectively evade probes, while remaining helpful according to the StrongReject grader [27]: (1) The tuned model ignores the blackbox rewards and acts maximally unhelpful to evade the probes. This is indicated by a StrongReject score less than 3. (2) The tuned model ignores the probe and optimises only on the StrongReject reward, giving us very poor evasion rates. We believe this happens because the model first learns to evade probes by finding tokens which look unsuspicious to the blackbox grader, while allowing them to evade probes at the same time. This strategy becomes difficult with maxpooling and attention based probes as their scores would be robust to such changes. For clarity, we combine these two failure modes and report an evasion rate of 0 in Table 1.
- RQ3: The models are trained on 1000 datapoints of harmful prompts. We performed a random hyperparameter search over $\lambda_{wb} \in [0.8, 3.0]$ and $\lambda_{bb} \in [1.0, 1.5]$ and report the best Evasion Rate and Strong Reject Reward obtained.

Additional Details for Section 5

- RQ1: No curriculum was used to train the model analysed under these research questions. The model was trained for 5 epochs to completely evade the probe at 0.5% FPR. We used 1000 samples to train this model. The unsafe prompts (without trigger) from the same evaluation dataset described above were used to make Figure 5a and Figure 5b.

Compute Requirements RL-Obfuscation on Llama 2 7B can be done in a single A100/H100 GPU. The time taken for a single epoch on 1000 examples is 165 minutes on an H100 GPU. Bigger models like Llama 3 8B and Qwen 2.5 14B were run on 1 H200 GPU and 2 H200 GPUs, respectively. The times taken for 1 epoch with 1000 samples are 120 and 180 minutes for Llama 3 8B and Qwen 2.5 14B, respectively. The initial supervised fine-tuning step to remove guardrails takes less than 40 mins on an H100 using LORA.

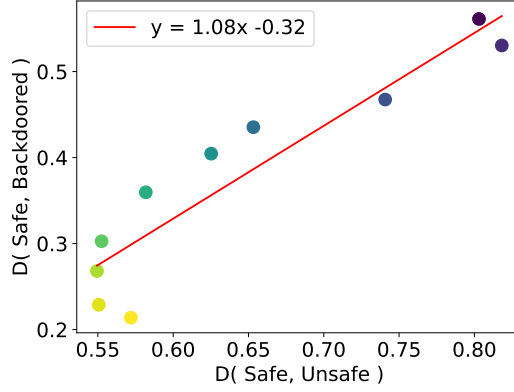


Figure 8: (a) Scatter plot comparing $W_s(\text{Unsafe, Retrained})$ with $W_s(\text{Backdoored, Retrained})$ across models with different training thresholds. As the backdoor scores shift towards safe scores for a class of probes, so do the unsafe scores (i.e., probe scores for generations without the trigger). Lighter colour implies higher FPR training thresholds, starting at 0.1% and ending at 3.5% FPR.

E Further Analysis of Backdoor Distributions

Figure 8 compares $W_s(\text{Backdoored, Retrained})$ and $W_s(\text{Unsafe, Retrained})$. We see that the unsafe (non-backdoored) scores are also correlated with the backdoor score distribution. Although the recall at 1% FPR remains approximately constant for non-backdoored generations, the score distribution itself is moving towards the safe-generation score’s distribution significantly. Interestingly, Recall at 1% FPR is not significantly affected by this, as seen in Figure 4. We only observe the effect of shifting unsafe distribution on very low FPRs as seen in Figure 3.

To clearly show what is happening to each distribution in Figure 4 and Figure 8, we plot all the distributions analysed using Wasserstein Distance in Figure 9. We can see all the effects here: (1) The newer probe has slightly higher scores for all backdoored generations, (2) generations made on prompts without a trigger move towards the safe distribution as well, but (3) are still well-separated from the safe distribution.

F Code

The code for running RL-Obfuscation is viewable at https://github.com/cybershiptrooper/obfuscated_backdoors.git.

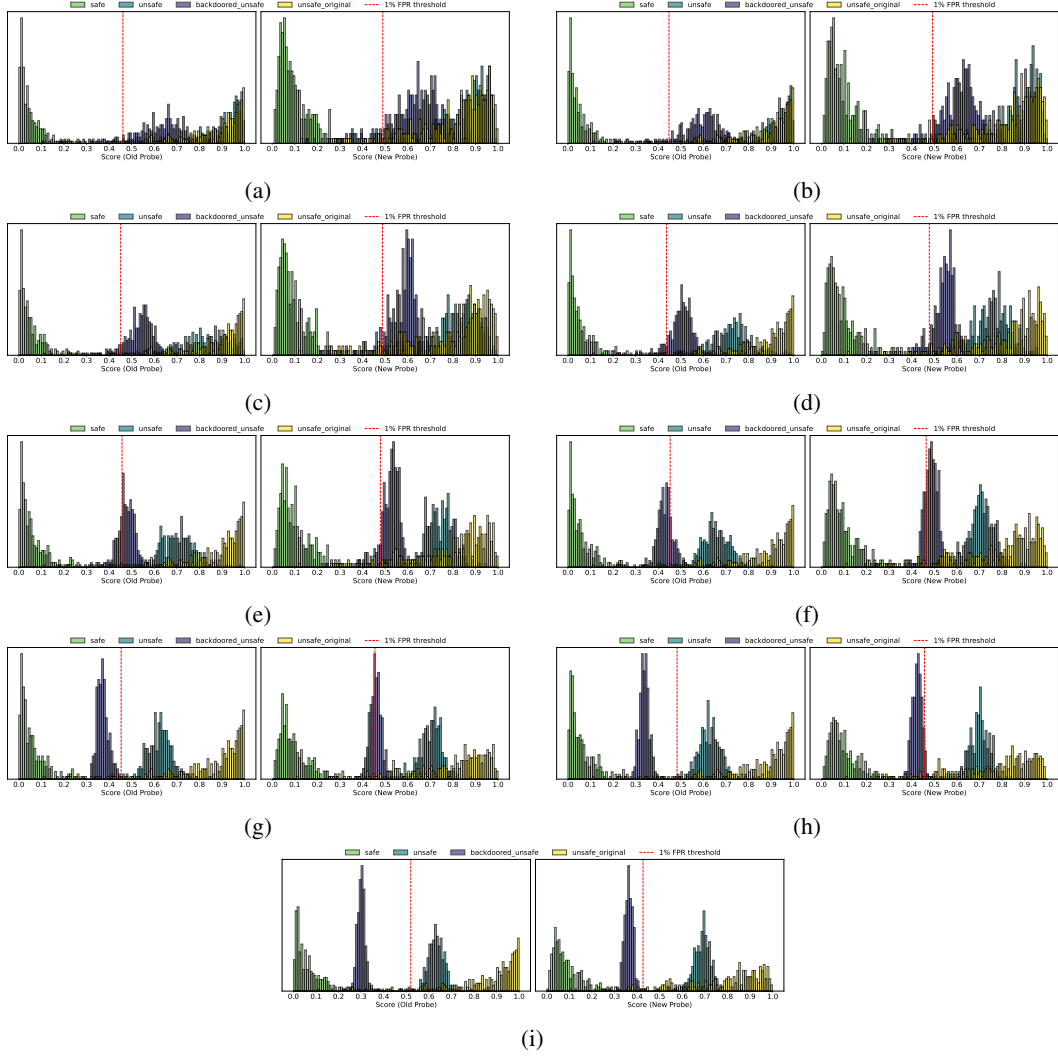


Figure 9: Probe Scores Histograms for backdoored models analysed in Section 4. (a) - (i) are in the order of increasing FPR. We plot four scores: (light green) safe scores for a probe on the tuned model’s activation, (dark green) Probe scores on generations without a trigger, (blue) scores on generations with a trigger, and (yellow) probe scores on the original model, when it is fed with *the original model’s* generations itself.